Available online at www.sciencedirect.com
SCIENCE DIRECT
Carbon 44 (2006) 638–645
CARBON
www.elsevier.com/locate/carbon

Analysis of the microporous texture of a glassy carbon by adsorption measurements and Monte Carlo simulation. Evolution with chemical and physical activation

M. Pérez-Mendoza [a,*], C. Schumacher [b], F. Suárez-García [c], M.C. Almazán-Almazán [a], M. Domingo-García [a], F.J. López-Garzón [a], N.A. Seaton [b]

[a] Departamento de Química Inorgánica, Facultad de Ciencias, Universidad de Granada, E-18071 Granada, Spain
[b] Institute for Materials and Processes, School of Engineering and Electronics, The University of Edinburgh, The King's Buildings, Edinburgh EH9 3JL, UK
[c] Departamento de Química Inorgánica, Universidad de Alicante, Apartado 99, E-03080 Alicante, Spain

Received 2 June 2005; accepted 28 September 2005
Available online 15 November 2005

Abstract

A mesoporous glassy carbon has been chemically (KOH) and physically (CO_2) activated in order to improve its micropore volume while preserving the well-defined mesopore network. The microporosity of the glassy carbon and the evolution of the micropore texture with activation have been studied by means of Monte Carlo simulation and gas adsorption. Micropore size distributions obtained from simulated adsorption isotherms on slit-shaped pores revealed different accessibilities of methane and nitrogen to the microporous texture of the original sample, indicating the presence of constrictions in the micropore network. Both activating agents are able to increase the micropore volume generating new micropores, although KOH showed to be more effective. While CO_2 treatment preserved some hindrances to the access of nitrogen molecules to the micropores, KOH activation generates a more accessible micropore network. Therefore, chemical activation by KOH is a suitable way to increase the adsorption capacity of glassy carbons while preserving the mesoporous structure. Molecular simulation of adsorption linked to experimental adsorption of different gases, has proven to give very satisfactory results in analysing the evolution of the micropore texture and accessibility of carbon materials by different activation treatments.

Keywords: Glass-like carbon; Activation; Molecular simulation; Adsorption; Microporosity

1. Introduction

Carbon materials with different characteristics are often used in adsorption-related processes such as gas separation, purification and storage, or as catalyst supports [1]. These potential uses as adsorbents or catalyst supports come from a well-developed internal porosity and from the possibility of modifying the textural and surface properties of carbon materials by simple post-treatments. Most of the carbon materials used in such applications are activated carbons which have a wide distribution of pore sizes generated during the activation step [2]. Nevertheless, for certain applications it is desirable to have materials with a controlled pore size distribution (PSD) which can improve the selectivity towards certain adsorptives.

In particular, glassy carbons are carbon materials prepared by slow pyrolysis of organic polymers and copolymers such as polyfurfuryl alcohol, phenol-formaldehyde or acetone-furfural. They present many interesting features that are not common to other carbon materials. Low density, high chemical inertness, high resistance to oxidation and hardness can be cited among them. Thus, the special characteristics allow these materials to be useful in different technological applications that range from reinforcement materials to electrodes [3–5]. One of the most important

* Corresponding author. Tel.: +34 9582 43 235; fax: +34 9582 48 526.
E-mail address: mjperezm@ugr.es (M. Pérez-Mendoza).

0008-6223/$ - see front matter © 2005 Elsevier Ltd. All rights reserved.
doi:10.1016/j.carbon.2005.09.037

characteristics of glassy carbons, which adds extra versatility to these materials, is the possibility of "tailoring" their porous texture depending on the preparation conditions and on the raw material [4,6,7]. Nevertheless, they do not present a well-developed microporosity, although they can have a substantial and homogeneous mesoporosity [8,9]. In order to improve the potential applications of glassy carbons as molecular sieves, adsorbents or catalysts supports, it is desirable to increase the micropore volume while preserving the well-defined mesopore network, rendering materials with an enhanced adsorption capacity and improved selectivity. This task is not as straightforward as in other carbon materials due to the above-mentioned chemical inertness and hardness that characterize this kind of materials.

This work studies the textural characteristics of a mainly mesoporous glassy carbon obtained from pyrolysis of polyfurfuryl alcohol, and the development of its microporous texture by physical (CO_2) and chemical (KOH) activation methods. The effect of such treatments on the porous network is studied by adsorption of different gases (N_2, CO_2, CH_4, C_2H_6) and by grand canonical Monte Carlo (GCMC) simulations. Monte Carlo simulation in the grand canonical ensemble is a suitable method, which has proven to give very satisfactory results, to simulate and predict the adsorption behaviour of porous solids once a model pore system has been provided [10,11]. Moreover, the use of simulated isotherms on model pores of varying sizes can provide a reliable way to obtain representative pore size distributions of different kinds of solid adsorbents [12,13]. The results from molecular simulation will be contrasted with the experimental adsorption data to draw out conclusions about the accessibility of the microporosity generated by activation to the different adsorptives under study.

2. Experimental

The preparation of the glassy carbon, denoted as P3M, has been previously described [8,14]. It can be summarized as the polymerization of furfuryl alcohol followed by further carbonization at very low heating rate up to 773 K. Triton X-100 was used as dispersing agent. Although the use of a pore former is a common practice in the preparation of these materials, no pore former was added in this case as a material with substantial and homogeneous mesoporosity can be obtained without it [8]. Two different activation methods were studied: physical and chemical. The physical activation was carried out in a horizontal furnace using CO_2 as activating agent (100 ml min^{-1}) at 1073 K for 4 h. The sample was heated up to the activation temperature and cooled down in a nitrogen atmosphere. KOH was used for chemical activation. The glassy carbon was suspended in a KOH solution (KOH:C 1:1) for 72 h in an inert atmosphere. The suspension was then evaporated in rotary evaporator and dried. The carbon material was further pyrolysed at 1073 K for 4 h in a nitrogen flow (100 ml min^{-1}). The activated samples are denoted P3M-CO_2 and P3M-KOH depending on the activating agent employed.

The porous texture of the samples was analysed by physical adsorption of nitrogen, CO_2, ethane and methane. N_2 adsorption (99.999% pure) was measured at 77 K in a volumetric adsorption apparatus, ASAP 2010 (Micromeritics). The N_2 isotherms were analysed according to the BET method to calculate the specific surface area, S_{BET} (area of nitrogen molecule: 0.162 nm^2 [15]) and the α_S method (using Spheron 6 carbon black as reference material) to calculate the external (or non-microporous) surface area (S_{ext}) and the micropore volume ($V_{\mu p}$). CO_2 adsorption was carried out in a volumetric system at 273 K. The micropore volume (W_0) and the surface area accessible to CO_2 (S_{CO_2}) molecules were determined using the Dubinin–Radushkevich equation and assuming a molecular area of 0.187 nm^2 [16].

The equilibrium methane and ethane isotherms up to high pressure were determined using a bench scale adsorption/desorption apparatus, which has been previously described in detail [17]. Around 5 g of sample were outgassed to 10^{-3} Torr at 423 K for at least 3 h prior to the experiments. The Peng–Robinson equation of state was used for the calculation of the number of moles in the gas phase. The adsorptive gases (99.99%) were supplied by BOC Co. and dried before introducing them into the system. A description of the method employed to measure pure gas adsorption isotherms in this system is also reported in Ref. [17]. The uncertainty in the data obtained is estimated to be less than 0.2%.

Mercury porosimetry up to 412 MPa was used to determine the pore size distribution of pores wider than 3.6 nm, following Washburn's equation. The measurements were carried out in a Quantachrome Model Autoscan 60.

3. Molecular simulation of gas adsorption

Monte Carlo simulation in the grand canonical ensemble (GCMC) provides a very powerful tool for studying fluid adsorption on porous materials as the chemical potential (related to the bulk pressure by an equation of state), the temperature and the volume are kept constant while the number of molecules in the adsorbed phase is allowed to fluctuate, as in a real adsorption experiment. It is a statistical–mechanical method that rigorously solves a molecular level model by generating a succession of molecular configurations, each characteristic of equilibrium. This is done by generating trial configurations by moving, adding and deleting molecules and accepting each trial probabilistically according to the appropriate Boltzmann factor [10,11]. The number of molecules per unit volume of pore space can be obtained by averaging over the configurations generated. Therefore, the method only depends on the realism of the adsorbate–adsorbent and adsorbate–adsorbate interactions used as inputs, as no approximations are made in the solution of the statistical–mechanical model.

In order to obtain the PSD of the P3M materials, the adsorption isotherms of nitrogen, methane and ethane in slit pores of various widths were computed by GCMC simulation. The model pores consist of a rectangular unit cell containing a three-layered planar wall of graphitic carbon with hexagonal structure of well-crystallized graphite (ABA stacking sequence) and with a layer separation in the x,y-plane of 0.335 nm [18]. This unit cell has periodic boundary conditions in the x and y direction to obtain a wall that is effectively infinite in these directions. Slit pores of the desired width (from 0.3 to 4.2 nm) were constructed by applying the corresponding unit cell size and periodic boundary conditions in the z direction. [An alternative approach to the generation of model porous carbons is to use reverse Monte Carlo simulation [19,20]. This approach gives model structures that, unlike the independent-pore model described above, are broadly consistent with a range of structural characteristics of real carbons, including X-ray and neutron diffraction data, as well as adsorption data. However, models of this type are not readily tuned to adsorption data for particular real carbons, and so are not suitable for the present purpose.]

The van der Waals interactions between gas molecules and adsorbent are represented by Lennard-Jones potentials. To obtain the interaction parameters between different Lennard-Jones sites, the Lorentz–Berthelot combination rules were applied. Methane is modelled as a single Lennard-Jones site, while nitrogen and ethane molecules are modelled as two Lennard-Jones sites. The Peng–Robinson equation of state was used to relate the pressure of the system to the chemical potential. The carbon atoms of the two graphitic surface layers of the pore wall are represented explicitly. In order to reduce the computation time, the middle layer is modelled as a plane of "smeared-out" carbon atoms with the density of graphite, according to the approach of Steele in [21]. Thus, its interaction with a gas molecule can be calculated in a single integral instead of a sum over a large number of interactions with explicit carbon atoms. The Lennard-Jones parameters applied and the bond length of the two-site molecules and the graphitic planes are listed in Table 1 [21–24]. A snapshot of the simulation of nitrogen adsorption in one of the model pores is represented in Fig. 1 as an example. The simulated nitrogen isotherms for model pores of different sizes are shown in Fig. 2. Most of the sizes studied have been omitted for the sake of clarity.

Table 1
Lennard-Jones parameters and bond lengths used in the GCMC simulations

Site	σ [Å]	ε/k_B [K]	d [Å]
C (graphite) [21]	3.400	28.0	1.420
CH_4 (methane) [22]	3.810	148.2	–
CH_3 (ethane) [23]	3.512	139.8	2.353
N (nitrogen) [24]	3.310	37.3	1.090

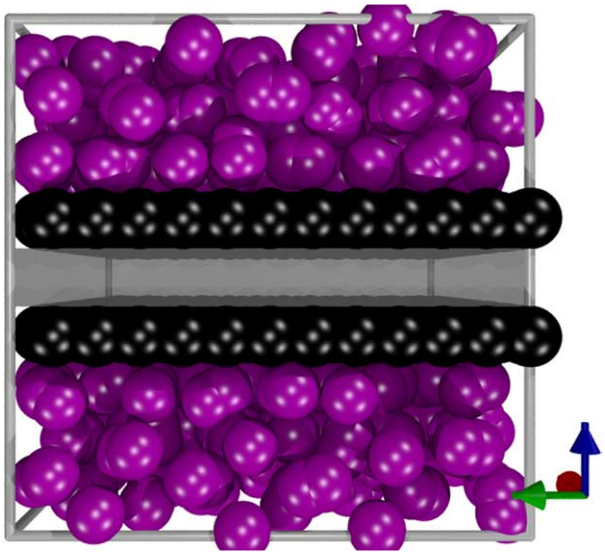

Fig. 1. Snapshot of the simulation of nitrogen adsorption (100 kPa). Dark spheres correspond to carbon atoms. The middle carbon layer is modelled as a plane of "smeared-out" carbon atoms with the density of graphite.

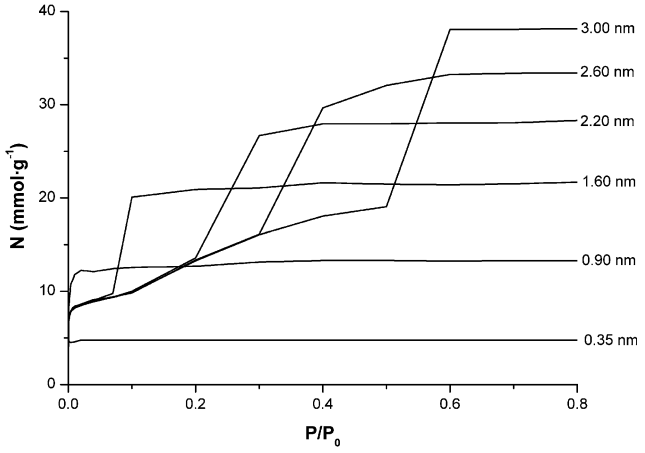

Fig. 2. Simulated nitrogen adsorption isotherms on model pores of different sizes. Most of the sizes have been omitted for the sake of clearness.

4. Results and discussion

4.1. Porous texture analysis of P3M

As mentioned above, the textural characteristics of the glassy carbon P3M, used in this study as the starting material, were analysed by means of gas adsorption and GCMC simulation. Other characterization results regarding the chemical surface characteristics of this material are available in the literature [25]. Fig. 3 shows the experimental nitrogen adsorption isotherms on the different samples used in this study.

Regarding the original sample P3M, the nitrogen adsorption isotherm can be classified as a hybrid between types I and IV (according to the IUPAC classification). This is an indicator of the presence of both micro- and

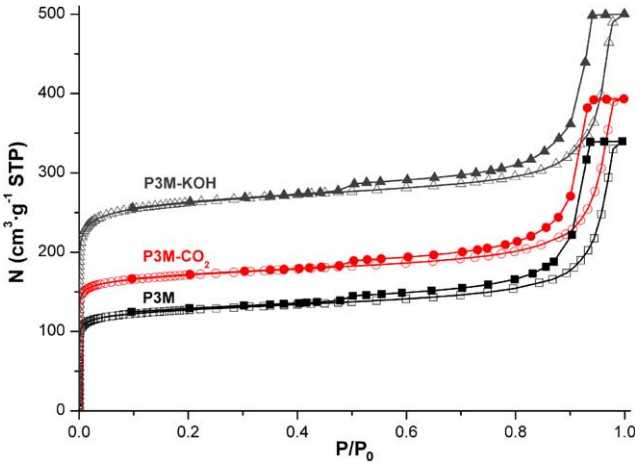

Fig. 3. Experimental nitrogen adsorption isotherms at 77 K. Solid symbols represent desorption branches.

mesopores. Furthermore, the relatively narrow hysteresis loop at high relative pressures, with adsorption and desorption branches being almost vertical and nearly parallel is characteristic of a narrow size distribution of mesopores.

The PSD of pores larger than 6 nm (which covers the upper part of the mesopore region) was obtained from mercury porosimetry following Washburn's equation (Fig. 4). As this PSD is obtained from mercury injection, it is not the true PSD of the mesopores, but rather reflects the percolative nature of the mercury injection process. The peak in the mercury PSD, which represents the pore size at which mercury percolates the sample, is around 19 nm for P3M and is larger for KOH the activated sample, showing that the size of the mesopores is slightly increased by this activation process. This point will be addressed in the next section. The total mesopore volume measured by this technique for sample P3M reaches 0.44 $cm^3\ g^{-1}$ (Table 2). There is no evidence of significant macroporosity, the presence of which would be indicated by a second peak in the mercury PSD, emphasizing the highly mesoporous nature

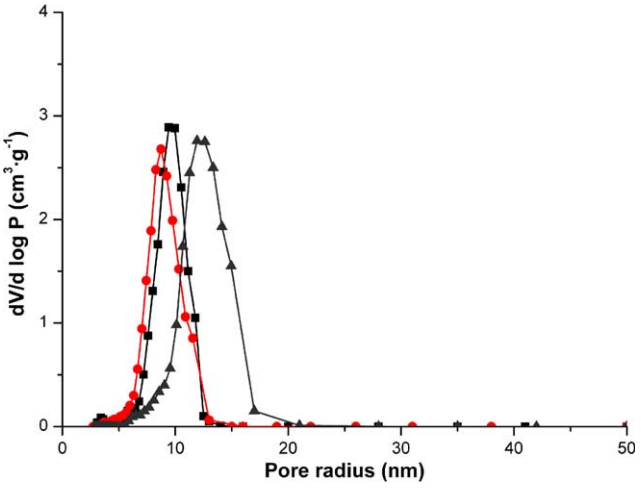

Fig. 4. Mesopore size distributions of samples P3M (■), P3M-CO_2 (●) and P3M-KOH (▲) obtained from mercury porosimetry.

of this material. A summary of the textural parameters of P3M and activated samples is given in Table 2.

As can be deduced from the table, the P3M sample has a well-developed porosity with a nitrogen S_{BET} of 484 $m^2\ g^{-1}$. Nevertheless, the different values of micropore volumes ($V_{\mu p}$ and W_0) and specific surface areas measured by N_2 and CO_2 adsorption (S_{BET} and S_{CO_2}), higher for the latter, suggest the presence of a narrow microporosity not accessible to the nitrogen molecules due to lower kinetic energy of this molecule at the temperature of adsorption.

PSD-based models are frequently used to describe the internal structure of carbon materials [12,26–30]. In this case, a micropore PSD to describe adsorption on sample P3M was obtained from the nitrogen simulated and experimental isotherms following the implementation of Davies and Seaton [12]. It is based on solving the adsorption integral equation:

$$N(P_i) = \int_0^\infty \rho(w, P_i) f(w)\, dw \quad i = 1, \ldots, n \tag{1}$$

where $N(P_i)$ is the experimental amount adsorbed at pressure P_i, $\rho(w, P_i)$ is the adsorption density in a model pore of a diameter w, $f(w)$ is the pore size distribution, and n is the total number of adsorption measurements used in the analysis. Once the simulated isotherms are known, this equation can be solved by numerical inversion to obtain a PSD that fits the experimental data. The method adopts a discrete representation of the PSD and, thus, the PSD obtained is not constrained to any form. A complete description of the method and the implications inherent to solving Eq. (1) to obtain a PSD can be found in Refs. [12,26]. The proposed PSD is shown in Fig. 5, where n represents the number of pores, i.e., defined as a pore number distribution.

The fit of the simulated isotherm obtained using such PSD to the experimental data is shown in Fig. 6. Pressure has been plotted using a logarithmic scale for better representation of the low pressure region. As can be observed, there is very good agreement between the experimental and calculated isotherm. The PSD shows a high number of narrow micropores, with the maximum centred on 0.7 nm.

As the PSD is a structural feature of the solid, if the PSD of P3M depicted in Fig. 5 is a good representation of the pore structure of the material, it should be able to predict adsorption from simulated isotherms at different conditions, i.e., different temperatures or gases, using Eq. (1) with the same PSD. Adsorption data up to high pressure of ethane at 298 K and methane at 263 K have been used to test the PSD obtained from nitrogen adsorption. The predictions using this PSD and the experimental data for ethane and methane adsorption are shown in Fig. 7.

As can be observed, the adsorption is very slightly underpredicted at low pressures in the case of ethane, while there is very good agreement at high pressure. Methane adsorption, however, is considerably underpredicted. This suggests that methane has access to porosity in the real

Table 2
Textural parameters

Sample	S_{BET} ($m^2\ g^{-1}$)	S_{ext} ($m^2\ g^{-1}$)	$V_{\mu p}$ ($cm^3\ g^{-1}$)	S_{CO_2} ($m^2\ g^{-1}$)	W_0 ($cm^3\ g^{-1}$)	V_{meso}[a] ($cm^3\ g^{-1}$)	S_{sim}[b] ($m^2\ g^{-1}$)
P3M	484	90	0.16	675	0.24	0.44	195
P3M-CO2	663	100	0.22	755	0.27	0.44	341
P3M-KOH	1012	104	0.36	905	0.32	0.44	496

[a] From mercury porosimetry.
[b] Surface area calculated from simulation of nitrogen adsorption.

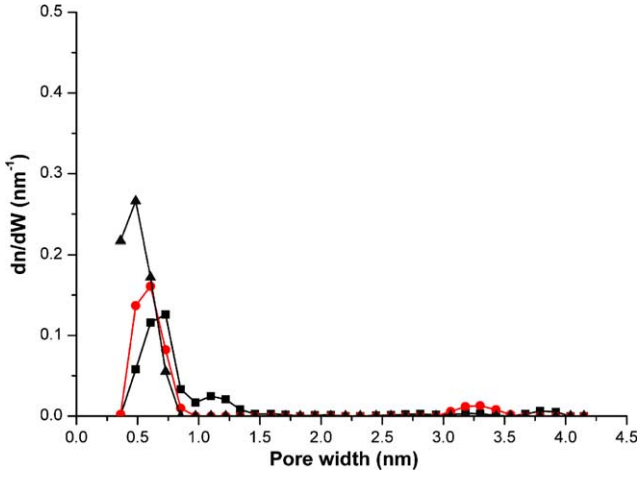

Fig. 5. PSDs obtained from N_2 adsorption at 77 K (■), C_2H_6 at 298 K (●) and CH_4 at 263 K (▲) on P3M.

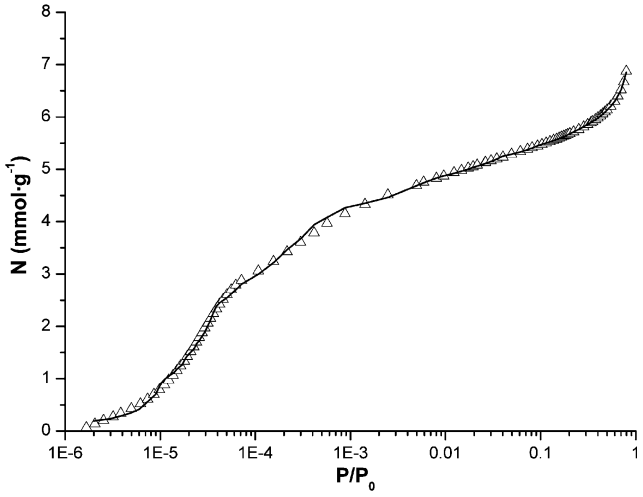

Fig. 6. Fitting of simulated N_2 adsorption isotherm (line) to experimental adsorption data (symbols) at 77 K on sample P3M.

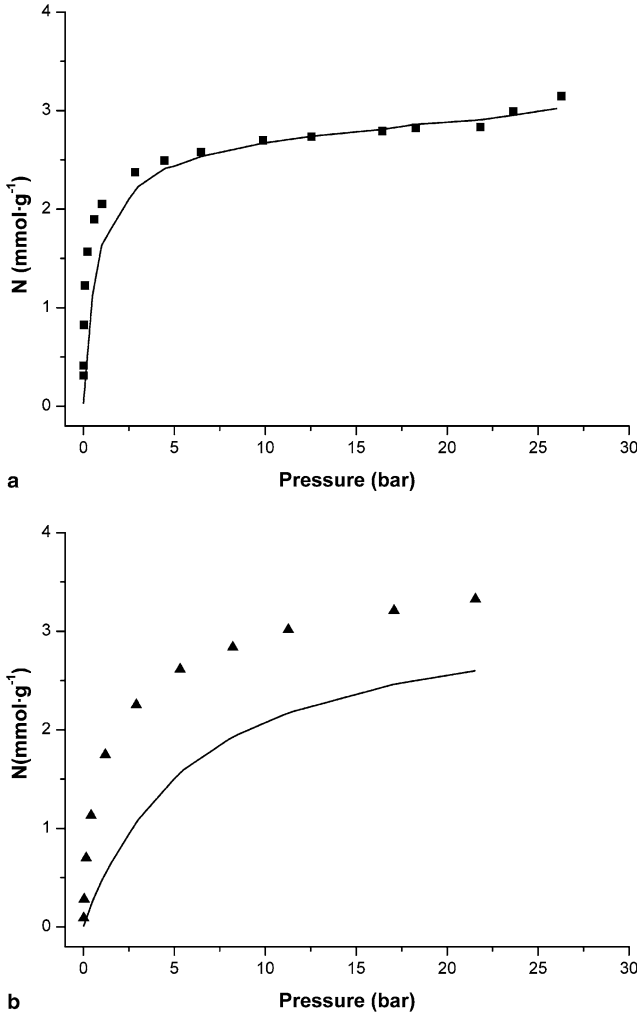

Fig. 7. Predicted (lines) and experimental (symbols) adsorption isotherms of ethane at 298 K (a) and methane at 263 K (b) on sample P3M.

material that is not accounted for in the PSD obtained by analysing nitrogen adsorption. In other words, it seems that methane has access to porosity not accessible to nitrogen.

The different accessibility of the gases to the porosity can be used to draw out new conclusions on the microporosity of the P3M material. We have calculated the PSD using the two other adsorptives, in the same way we did for nitrogen. The PSDs obtained using all three different adsorptives are shown in Fig. 5. It is clear that, although the PSDs have similar shapes, the micropore volume accessible to the different species (the integral of the PSD up to 2 nm) varies. In particular, methane is able to penetrate a larger micropore volume than nitrogen and ethane due to its smaller size (0.11 $cm^3\ g^{-1}$ for methane and 0.08 and 0.07 $cm^3\ g^{-1}$ for nitrogen and ethane, respectively), pointing out the presence of hindrances to the access of nitrogen and ethane molecules to a certain microporosity volume. This is in agreement with the former conclusion about the existence of a narrow microporosity inaccessible to

nitrogen, deduced from the experimental nitrogen and CO_2 adsorption data (Table 2).

These results can be understood by introducing percolation concepts. The carbons contain networks of interconnected pores, possibly with constrictions at the pore entrances or within individual pores. If it is within a certain size range, a particular constriction might permit the passage of methane, whilst preventing the passage of the larger ethane and nitrogen molecules. (Although the size of the Lennard-Jones site that forms the methane molecule in the simulations is larger than the Lennard-Jones sites in the ethane and nitrogen molecules, the greater length of the ethane and nitrogen molecules makes them less likely to pass through constrictions.) As a result, the ethane and nitrogen molecules might be excluded from some pores that are nevertheless large enough to contain them. Furthermore, some of the pores from which the nitrogen and ethane are excluded might not themselves be near constrictions; rather, the operative constrictions might be some distance away in the pore network. This percolation effect has been observed for microporous carbons [31] as well as for zeolites [32] and periodic mesoporous silicas [33]. If it is considered that differences in accessibility have been found in ordered materials and in microporous carbons which have a more ordered structure than glassy carbons [1,5], the results found for P3M material are far from unexpected and accessibility problems in this type of materials can be relevant and likely to occur. [We note in passing that Davies and Seaton [34] found a significant connectivity effect in the adsorption of methane and ethane on BPL carbon (a graphitizable carbon); however the experimental data on which this conclusion was based were subsequently shown to be in error, and the actual adsorption behaviour of this material [35] shows no connectivity effect for methane and ethane.]

4.2. Evolution of porosity with activation

As has been already suggested, it would be interesting to develop the microporosity of glassy carbons while preserving their unimodal distribution of mesopores. Due to the chemical inertness of these materials, the activating agent has to be reactive enough to produce textural changes in the sample but in a controlled way. In this study, both physical and chemical activation have been studied. In the former case, CO_2 has been used, while in the second KOH was the activating agent. Activation by CO_2 is a well-known method to activate carbon materials and has been thoroughly studied. It progresses by consumption of carbon material generating CO through an endothermic reaction [2]. In contrast, KOH activation is not so well studied. Nevertheless, there seems to be agreement that the activation occurs by intercalation of potassium ions between the micrographene layers, distorting and consuming part of them, and hence generating new porosity [36–38].

In relation to what has been previously commented regarding the mesoporosity analysis by mercury intrusion, it is clear from Fig. 4 that CO_2 activation is not modifying substantially the mesopore network but rather is just displacing the distribution to slightly lower pore sizes. In the case of KOH, there is a widening effect on the mesopores and as a consequence the maximum of the distribution is shifted to 24 nm. Nevertheless, it is worth noting that the three samples present the same mesopore volume accessible to mercury under pressure, as can be deduced from the data in Table 2. This suggests that the activations are not generating any new mesoporosity and they are just modifying the existing mesopore network, only slightly in the case of CO_2 and more markedly in the case of chemical activation. Fig. 3 shows that the hysteresis loops observed at high pressure are nearly identical for the three samples. Therefore it can be concluded that both activations preserve the original mesopore structure of the sample, with neither substantial changes to the mesopores, nor creation of new mesopores, although it has to be borne in mind that KOH activation widens the distribution. It has to be recalled that the aim pursued with these activations was to increase the microporosity while largely preserving the mesopore structure.

Since both activations seem to succeed in not destroying the mesopore network, it remains to analyse if they are also able to increase the micropore volume and the adsorption capacity. From an analysis of the experimental nitrogen adsorption isotherms in Fig. 3, it can be clearly deduced that there is a substantial development of the microporosity for the activated samples. This increase of adsorption in the region of micropore filling, i.e., at low relative pressures, is more remarked in the case of chemical activation with KOH. The volume of micropores calculated by the α_s method increases from 0.16 $cm^3\,g^{-1}$ for the original sample to 0.22 and 0.36 $cm^3\,g^{-1}$ for samples P3M-CO_2 and P3M-KOH, respectively (Table 2). In the same way, the specific surface area accessible to nitrogen (S_{BET}) also increases drastically, being for P3M-KOH more than twice that for original sample P3M. The specific surface areas and micropore volumes obtained by applying the Dubinin–Raduschkevich equation to the CO_2 adsorption data do not show such a high increase in microporosity. Nevertheless, the comparison of nitrogen and CO_2 adsorption data can shed some light on how the development of the micropore network in the activated samples takes place. In the original sample, the microporosity is more accessible to CO_2, as can be deduced from S_{CO_2} and W_0 values in comparison to those from nitrogen adsorption, and as was explained in the former section. The sample activated with CO_2, P3M-CO_2, maintains the higher accessibility towards the CO_2 adsorptive molecules, although the values of the surface areas and micropore volumes are closer to those from nitrogen adsorption. Thus, it seems that CO_2 activation produced new narrow micropores, or at least made more micropores accessible to both adsorptives. In contrast, the trend changes for the sample activated with KOH, which presents higher micropore volume and specific surface area from N_2 than from CO_2 adsorption, indicating the enlargement of the existing micropores and the

development of new wider microporosity. This results in a higher proportion of supermicropores not evaluated by CO_2 adsorption due to the limited relative pressure of the adsorption experiment (atmospheric pressure). Under this conditions, CO_2 is known not to adsorb in pores larger than 1 nm [39] while nitrogen adsorption can take place even in small mesopores [40].

PSDs from simulated and experimental nitrogen adsorption isotherms for the activated samples have also been obtained following the same method [12] applied to P3M in the former section. The results so obtained are shown in Fig. 8, together with that of the original sample for comparison.

The agreement between the predicted isotherms for the activated samples using such PSDs and the experimental ones is similar to that represented in Fig. 6 for the original sample. Again it is evident the substantial increase in the microporosity accessible to nitrogen produced in both activations (more important for the KOH activated sample), in good agreement with the data compiled in Table 2. Moreover, the greatest increase is found in narrow micropores, shifting the maximum of the distribution from 0.6 nm to sizes smaller than 0.5 nm. It has also to be noted that KOH activation produced a significant increase in the number of micropores larger than 1 nm, according to the calculated PSDs. The condensation of nitrogen in such supermicropores produces an overestimation of the surface area accessible to nitrogen if BET method is employed, rendering a high S_{BET} value presented by this sample (Table 2). More accurate values of the surface area accessible to nitrogen can be geometrically calculated from the PSDs obtained from the simulated isotherms of nitrogen adsorption (Table 2). According to these figures, P3M-KOH sample presents a surface area 2.5 times higher than P3M, while the increase in not as drastic for the sample activated by CO_2.

In the same way as before for the P3M sample, a PSD obtained with another adsorptive can give further insight to P3M-KOH microporosity. For this purpose, methane

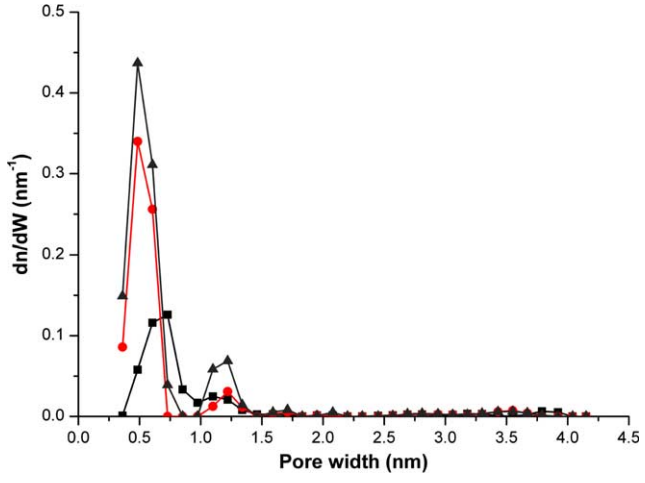

Fig. 8. PSDs obtained from N_2 adsorption at 77 K for samples P3M (■), P3M-CO_2 (●) and P3M-KOH (▲).

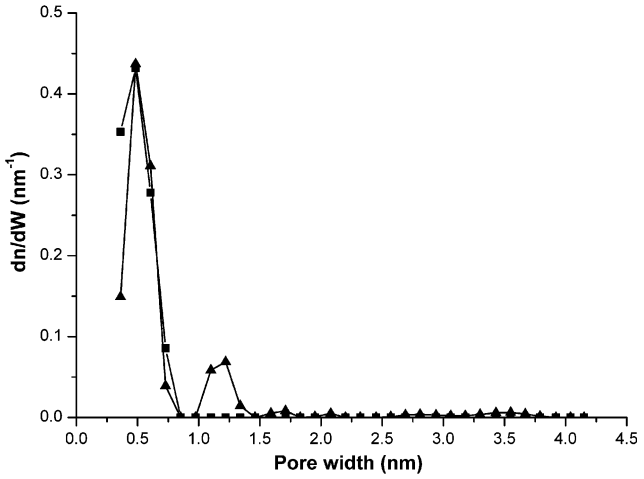

Fig. 9. PSDs obtained from N_2 adsorption at 77 K (▲) and CH_4 at 263 K (■) for sample P3M-KOH.

experimental and simulated isotherms at 263 K on this sample were employed to obtain a new PSD (shown in Fig. 9 together with that obtained from nitrogen for comparison). In contrast to what is observed for the original sample (Fig. 5), methane and nitrogen adsorptives in the KOH activated one have access to the same microporosity, rendering very similar PSDs except for the smallest pore size (due to the clear smaller effective size of methane molecules) and for pores larger than 1 nm, where methane adsorption is so weak that it is almost independent of the pore size, so that the methane-derived PSD in this range is unreliable. Therefore, this corroborates the hypothesis that KOH is widening the microporosity and clearly eliminating the constrictions which hindered nitrogen adsorption to an important extent in the original sample (as was demonstrated in the former section), and which was proposed based on data given in Table 2.

5. Conclusions

A mesoporous glassy carbon has been activated by physical (CO_2) and chemical (KOH) methods, in order to increase its adsorption capacity by developing the micropore volume while preserving its narrow mesopore size distribution. The porous texture of the original and activated samples has been analysed by means of experimental gas adsorption, mercury porosimetry and GCMC simulation of gas adsorption. The microporosity analysis of the original sample by experimental and simulated adsorption revealed different accessibilities of methane, ethane and nitrogen, pointing out the existence of steric factors hindering the access of nitrogen and ethane molecules to certain parts of the microporosity, as revealed by the different micropore size distributions obtained. The activation with both agents preserved the narrow character of the mesopore size distribution while increasing the micropore capacity. CO_2 activation did not produce any substantial changes in the mesoporosity while KOH widened slightly

the distribution but without any increase in the mesopore volume. Regarding the microporosity, KOH is more effective than CO_2 in generating new accessible micropores and eliminating the constrictions hindering the adsorption of nitrogen molecules that are present in the original sample.

Acknowledgments

The authors acknowledge the financial support of Spanish Ministry of Education and Science (MEC project CTQ2004-07698-CO2-01/PPQ), Spanish Ministry of Environment (MMA expediente 033/2004/3), Junta de Andalucía and UK Engineering and Physical Sciences Research Council.

References

[1] Marsh H, Heintz EA, Rodriguez-Reinoso F. Introduction to carbon technologies. Alicante: Secretariado de Publicaciones, Universidad de Alicante; 1997.
[2] Bansal RC, Donnet JB, Stoeckli F. Active carbon. New York: Marcel Dekker; 1988.
[3] Lee SM. International encyclopedia of composites. New York: Wiley-VCH; 1989.
[4] Oya A. In: Marsh H, Heintz EA, Rodriguez-Reinoso F, editors. Introduction to carbon technologies. Alicante: Secretariado de Publicaciones, Universidad de Alicante; 1997. p. 561–95.
[5] Kinoshita K. Carbon: electrochemical and physicochemical properties. New York: Wiley; 1988.
[6] Rodriguez-Reinoso F. In: De Patrick JW, editor. Porosity in carbons: characterization and applications. London: John Wiley & Sons Inc.; 1995. p. 253–90.
[7] Radovic LR, Rodriguez-Reinoso F. In: Thrower PA, editor. Chemistry and physics of carbon, vol. 25. New York: Marcel Dekker; 1996. p. 243–358.
[8] Domingo-Garcia M, Lopez-Garzon FJ, Perez-Mendoza M. Modifications produced by O-2 plasma treatments on a mesoporous glassy carbon. Carbon 2000;38(4):555–63.
[9] Lopez-Garzon FJ, Domingo-Garcia M, Perez-Mendoza M, Alvarez PM, Gomez-Serrano V. Textural and chemical surface modifications produced by some oxidation treatments of a glassy carbon. Langmuir 2003;19(7):2838–44.
[10] Frenkel D, Smit B. Understanding molecular simulations: from algorithms to applications. San Diego: Academic Press; 2001.
[11] Allen MP, Tildesley DJ. Computer simulation of liquids. Oxford: Clarendon Press; 1989.
[12] Davies GM, Seaton NA, Vassiliadis VS. Calculation of pore size distributions of activated carbons from adsorption isotherms. Langmuir 1999;15(23):8235–45.
[13] Perez-Mendoza M, Gonzalez J, Wright PA, Seaton NA. Elucidation of the pore structure of SBA-2 using Monte Carlo simulation to interpret experimental data for the adsorption of light hydrocarbons. Langmuir 2004;20(18):7653–8.
[14] Lopez-Garzon FJ, Pyda M, Domingo-Garcia M. Studies of the surface-properties of active carbons by inverse gas-chromatography at infinite dilution. Langmuir 1993;9(2):531–6.
[15] Rouquerol F, Rouquerol J, Sing KSW. Adsorption by powders and porous solids. London: Academic Press; 1999.
[16] Gregg SJ, Sing KSW. Adsorption, surface area and porosity. London: Academic Press; 1982.
[17] Yun JH, Duren T, Keil FJ, Seaton NA. Adsorption of methane, ethane, and their binary mixtures on MCM-41: experimental evaluation of methods for the prediction of adsorption equilibrium. Langmuir 2002;18(7):2693–701.
[18] Boehm HP. In: Eley DD, Pines H, Weisz PB, editors. Advances in catalysis, vol. 16. New York, London: Academic Press; 1966. p. 179–274.
[19] O'Malley B, Snook I, McCulloch D. Reverse Monte Carlo analysis of the structure of glassy carbon using electron-microscopy data. Phys Rev B 1998;57(22):14148–57.
[20] Pikunic J, Clinard C, Cohaut N, Gubbins KE, Guet JM, Pellenq RJM, et al. Structural modeling of porous carbons: constrained reverse Monte Carlo method. Langmuir 2003;19(20):8565–82.
[21] Steele WA. Physical interaction of gases with crystalline solids. 1. Gas–solid energies and properties of isolated adsorbed atoms. Surf Sci 1973;36(1):317–52.
[22] Hirschfelder JO, Curtiss CF, Byrd RB. The molecular theory of gases and liquids. New York: Wiley; 1966.
[23] Fischer J, Heinbuch U, Wendland M. On the hard-sphere plus attractive mean field approximation for inhomogeneous fluids. Mol Phys 1987;61(4):953–61.
[24] Murthy CS, Singer K, Klein ML, Mcdonald IR. Pairwise additive effective potentials for nitrogen. Mol Phys 1980;41(6):1387–99.
[25] Perez-Mendoza M, Domingo-Garcia M, Lopez-Garzon FJ. Carbon materials as catalysts for methylamines synthesis. Appl Catal A—Gen 2002;224(1–2):239–53.
[26] Davies GM, Seaton NA. Development and validation of pore structure models for adsorption in activated carbons. Langmuir 1999;15(19):6263–76.
[27] Yin YF, McEnaney B, Mays TJ. Dependence of GCEMC simulations of nitrogen adsorption on activated carbons on input parameters. Carbon 1998;36(10):1425–32.
[28] Olivier JP. Improving the models used for calculating the size distribution of micropore volume of activated carbons from adsorption data. Carbon 1998;36(10):1469–72.
[29] Nguyen C, Do DD. Simple optimization approach for the characterization of pore size distribution. Langmuir 2000;16(3):1319–22.
[30] Sweatman MB, Quirke N. Characterization of porous materials by gas adsorption at ambient temperatures and high pressure. J Phys Chem B 2001;105(7):1403–11.
[31] Lopez Ramon MV, Jagiello J, Bandosz TJ, Seaton NA. Determination of the pore size distribution and network connectivity in microporous solids by adsorption measurements and Monte Carlo simulation. Langmuir 1997;13(16):4435–45.
[32] Rees LVC, Berry T. Sorption of non-polar sorbates in Linde Sieve—A modified by the pre-sorption of ammonia, vol. 149. Soc of Chem Ind Conf on Molecular Sieves, 1967.
[33] Perez-Mendoza M, Gonzalez J, Wright PA, Seaton NA. Structure of the mesoporous silica SBA-2, determined by a percolation analysis of adsorption. Langmuir 2004;20(22):9856–60.
[34] Davies GM, Seaton NA. Predicting adsorption equilibrium using molecular simulation. Aiche J 2000;46(9):1753–68.
[35] He YF, Yun JH, Seaton NA. Adsorption equilibrium of binary methane/ethane mixtures in BPL activated carbon: Isotherms and calorimetric heats of adsorption. Langmuir 2004;20(16):6668–78.
[36] Raymundo-Pinero E, Azaïs P, Cacciaguerra T, Cazorla-Amoros D, Linares-Solano A, Beguin F. KOH and NaOH activation mechanisms of multiwalled carbon nanotubes with different structural organisation. Carbon 2005;43(4):786–95.
[37] Guo J, Lua AC. Textural and chemical characterizations of adsorbent prepared from palm shell by potassium hydroxide impregnation at different stages. J Coll Interf Sci 2002;254(2):227–33.
[38] Hu ZH, Vansant EF. Synthesis and characterization of a controlled micropore-size carbonaceous adsorbent produced from walnut shell. Micropor Mater 1995;3(6):603–12.
[39] Vishnyakov A, Ravikovitch PI, Neimark AV. Molecular level models for CO_2 sorption in nanopores. Langmuir 1999;15(25):8736–42.
[40] Fernandez-Morales I, Almazan-Almazan MC, Perez-Mendoza M, Domingo-Garcia M, Lopez-Garzon FJ. PET as precursor of microporous carbons: preparation and characterization. Micropor Mesopor Mater 2005;80(1–3):107–15.